Inflatable membrane mirrors for optical passband imagery

Aden B. Meinel, FELLOW SPIE
Marjorie P. Meinel, FELLOW SPIE
Jet Propulsion Laboratory
California Institute of Technology
Pasadena, California 91109

Author's address information (note that we are retired, On-Call, JPL):

Aden B. Meinel & Marjorie P. Meinel
1600 Shoreline Drive
Santa Barbara, California 93109
T: 805-965-4762
Fa:x: 805-957-0113
E-mail: ameinel@earthlink.net

Abstract Past investigations of membrane mirrors have led to the conclusion that they are not suitable for imaging in the visible. We re-examine this conclusion and discuss ways to circumvent the principal problems. A re-analysis of l'Garde measurements of a 6 um thick membrane mirror corrects earlier interpretations of the "W-curve" asymmetry. Correction of the classical Hencky aspheric shape of membrane mirror is necessary to upgrade them for use in visible passbands. The theory of variable membrane thickness in a radial direction is presented. A numerical integration is done and a unique quadratic radial variation of thickness found which corrects for the u^4 Hencky term. Two methods to fabricate such a membrane are presented.

Subject terms: space optics, inflatable membrane mirrors, visible passband inflatable mirrors.

1 Introduction

Inflated membrane mirrors consist of two thin circular membranes that are sealed on their periphery, attached to a tensioning ring and inflated to a pressure sufficient to produce the focal ratio required of the mirror. Such inflated mirrors have been used for various applications wherein low imaging acuity is sufficient; for instance, microwave antennae[1,2,3] and solar energy concentrators[4,5]. They were never contemplated for optical passband imaging where high acuity is required. The basic problem is that the shape of an inflated membrane is neither spherical nor parabolic. The profile of such a mirror has an up-turned periphery with regard to a sphere and hence is an oblate spheroid. Its shape is generally expressed by an even power series termed the Hencky curve, after the first person to explore such mirrors[6]. The resulting spherical aberration is serious and forces placing a secondary mirror for a Cassegrain configuration far from the prime focus, as shown in Fig. 1. Hence an unconventionally large secondary mirror is required. With renewed interest in the possibility of using inflation-deployed optics[7] in space systems it is appropriate to re-examine the issues surrounding the use of inflatable optics. The challenge to transform the Hencky curve into a paraboloid can be better appreciated by comparing it to a paraboloid. For convenience of comparison one can write the equations for a Hencky surface, a spherical surface and a paraboloid in similar form as:

$$z(u) = \frac{D}{64F^2}\left(u^2 + 0.1111u^4\right) \qquad \textit{Hencky} \qquad (1a)$$

$$z(u) = \frac{D}{64F^2}\left(u^2 + 0.0156u^4\right) \qquad \textit{Sphere} \qquad (1b)$$

$$z(u) = \frac{D}{64F^2}\left(u^2 + 0.0000u^4\right) \qquad \textit{Paraboloid} \qquad (1c)$$

The magnitude of the u^4 terms show how much downward warping of the outer edge of a inflated membrane mirror is required even to reach equality with a sphere, and still more to reach a paraboloid. To reach the surface shape for a Ritchey-Chretien primary the u^4 term would need to be slightly negative with respect to a paraboloid.

When a paraboloid is subtracted from measurements of inflated membranes the resulting curve has been termed a "W-curve." The published W-curves[8, 9, 10] usually have a large asymmetry that has been interpreted as indicating an asymmetry in the inflated shape of the membrane. In view of the acceptance of this asymmetry as being real it is important to re-

analyze the original measurements and apply the appropriate corrections for the metrology zero point.

2 Re-analysis of the l'Garde data

Cassapakis[11] of l'Garde has kindly provided us with the measurement data for a 900 mm diameter, 6 um thick Mylar membrane mirror having a central radius of curvature of 2070 mm. The customary way to present this data in graphical form is to subtract a best fit parabolic curve, which results in the "W-curve." Occasionally curves are shown to have the exact reverse, an "M-curve." This in all probability reflects whether a paraboloid is subtracted from the measured curve or vice versa. Two examples showing this asymmetry are shown in Fig. 2. We have added a straight, but tilted, line tangent to the minima of these W-curves. This tilt is familiar to opticists as being an artifact caused by a small error in the zero-point of the metrology system, producing an error generally termed "coma."

The data provided to us did not show this large an asymmetry, as shown in Fig. 3, and was corrected by a small shift in the r and z coordinates of the data. The sagitta vs. radial zone is shown with respect to a paraboloid. In Fig. 4 we show data for the 6 um Mylar membrane mirror. The sagitta vs. radial zone is shown at the top and the difference with respect to a paraboloid at the bottom. A line fitted through the points for the difference curve when superimposed but reversed shows a difference for the outer five data points.

To further explore potential differences in symmetry of the inflated membrane we compared the l'Garde data for two orthogonal azimuths across the mirror. Fig. 5 (top) shows the slopes vs radial zone. In Fig. 5 (bottom) we have subtracted the parabolic slope so that the residual shows only the third power and higher terms.

3 Analysis

To understand the above results we have taken the plotted data, formed its mirror image and superimposed the resulting two curves. In Fig. 6 we show the result for an azimuth across the mirror surface. The superimposed curves show excellent agreement between the curves on both sides of center to the scale of the drawing in Fig. 6. The difference between the two curves is 7 um rms, as shown at larger scale in Fig. 6 (bottom). A major part of this difference is due to terms in u^6, u^8 ... not included in the Hencky equation.

We next examined the curve data for an azimuth in the transverse direction. In Fig. 7 we show the measured membrane sagitta minus the same parabolic curve for the cuts in orthogonal directions. The direct + reversed superimposed curves agree excellently showing symmetry in each direction; however, the orthogonal azimuths are different as is shown in Fig. 7.

This difference means that the oblate ellipsoid is astigmatic and to a degree that would produce a serious image error. In an optical system a fixed wavefront corrector or adaptive surface down stream from a flawed primary mirror can correct the on-axis field of view for a serious wavefront error, such as astigmatism. The slope asymmetry from Fig. 8 would produce an astigmatic image 36.4 mm diameter at mean focus. The l'Garde data sheets do not indicate the orientation of this membrane, so this asymmetry effect is not necessarily the maximum.

Figs. 7 and 8 raise two possibilities. This difference between the two orthogonal azimuths can be caused by a difference between the elastic properties of the membrane in these two directions. It also could be caused by a thickness gradient across the width of the original Mylar membrane as a result of the process. It is clear that both must be controlled better in order to produce a membrane mirror suitable for optical passband applications.

Measurements at l'Garde[13] found that Mylar is indeed orthotropic, the modulus in orthogonal directions differing by 44%; further, that it varies from batch to batch. They found that Kapton E is very close to isotropic.

Our re-analysis showed a difference in both the constant and the coefficients of u^2 and u^4; namely,

$$z = 42.33(0.937u^2 + 0.068\ u^4) \text{ for azimuth \#1, and} \quad (2)$$

$$z = 42.17(0.884\ u^2 + 0.115\ u^4) \text{ for azimuth \#2.} \quad (3)$$

Note that the edge value in the l'Garde data is at x = 443.5 mm. We have fitted this power series to x = 400 since the effect of higher order terms becomes significant as the periphery of the membrane is approached.

The boundary conditions for an inflated membrane mirror are 1) that the periphery of the mirror is defined by a flat ring and 2) that the central depth of the curve is the same in orthogonal directions regardless of variation of E or t in these directions. These conditions are illustrated in Fig. 9. Fig. 9 (left) shows this difference in curvature, the low E direction

being flatter near the center and steeper near the periphery. This difference is a form of astigmatism different from that encountered in conventional optics. Fig. 9 (right) shows the contours for equal slopes where the axis switches 90° from the central to the peripheral regions. Correction for this type of astigmatism can not be done by conventional optical elements in the system. It can be done with a wavefront corrector at a pupil and by having the opposite form of astigmatism.

The observed ratio between the constant and the u^2 term for the orthogonal azimuths is 1.064. The relationship of z as a function of u depends on $1/t^{1/3}E^{1/3}$. Assuming that the membrane thickness is constant this would imply a difference in E of $1.064^3 = 1.20$. This is half of what l'Garde has reported for Mylar: a reasonable agreement inasmuch as the azimuth of the membrane with respect to fabrication direction was not noted in the data supplied to us. No information on possible thickness variation with azimuth in the 6 um membrane was provided.

To assess the angular error resulting from this difference in curve depth vs. radial zone we calculated slopes between adjacent depth measurements in the l'Garde data. In Fig. 8 we show the direct + reversed curves of the slopes minus the parabolic term for both azimuths superimposed. The differences in slopes are not as obviously different from each other as were the differences in the sagittae as shown in Fig. 6. In part this is because the plot is solely of the cubic and higher slope terms, but the slope differences between both azimuths are still considerable at 400 mm off-axis: $\Delta\alpha = 0.0088$ rad, or 29 arc minutes.

4 Variable thickness membrane mirrors

The equation for the central deflection, z, of a circular thin plate to that for a thin membrane can be written with the equation for the inverse central deflection as the sum of two standard terms: the bending mode and a stretching mode.

$$\frac{1}{z} = \frac{Et^3}{k_1 \mathrm{Pr}^3} + \frac{E^{\frac{1}{3}} t^{\frac{1}{3}}}{k_2 P^{\frac{1}{3}} r^{\frac{4}{3}}} \cdot \qquad (4)$$

6 Bending mode Stretching mode

Bending is dominant for a thin plate but stretching is dominant for a thin membrane. For an example for a thin plate we take $E = 10^5$, t = 10 mm, P = 100 and r = 450 mm, whence

$$\Delta T = \frac{\pi^2 D^2 \Delta z}{4gTz^2} \tag{19}$$

1/z = 4.94 + 0.0062, z = 0.202 mm deflection . (5)

For a membrane mirror we take E = 10^5, t = 0.01 mm, P = 0.005 and r = 450 mm, whence

1/z = 9.9e-05 + 0.0170, z = 58.0 mm. (6)

The large change in the u^4 term for an inflated membrane mirror to attain a parabolic shape is the requirement. One option for achieving this goal is a membrane of variable thickness as advocated by Breckinridge[14].

4.1 *Theory*

The shape of a thin circular plate of diameter D under uniform pressure P is given for $0 \le u \le 1$ to terms up to u^4 by

$$z = \frac{kP^{\frac{1}{3}} D^{\frac{4}{3}}}{E^{\frac{1}{3}} t^{\frac{1}{3}}} f(u) \tag{7}$$

where t is the thickness of the plate, E the modulus of elasticity and u = 2x/D, the fractional radial distance from the center of the membrane. For an inflated membrane of uniform thickness k = 0.248. Inserting the expression for f(u) to terms up to u^4 we obtain

$$z = \frac{0.248P^{\frac{1}{3}} D^{\frac{4}{3}}}{E^{\frac{1}{3}} t^{\frac{1}{3}}} \left[au^2 + (1-a)u^4 \right] . \tag{8}$$

For the classical Hencky equation a=0.9. The natural shape of an inflated membrane has higher order terms than u^4 because of an increasingly steeper upward slope near the periphery of the mirror.

Let us define the variation of membrane thickness as

$t = f(t,u) = t_0\{1 + Au^2 + Bu^4 + Cu^6 \ldots)$. (9)

$1/z = 4.94 + 0.0062$, $z = 0.202$ mm deflection (5)

For a membrane mirror we take $E = 10^5$, $t = 0.01$ mm, $P = 0.005$ and $r = 450$ mm, whence

$1/z = 9.9e\text{-}05 + 0.0170$, $z = 58.0$ mm. (6)

The large change in the u^4 term for an inflated membrane mirror to attain a parabolic shape is the requirement. One option for achieving this goal is a membrane of variable thickness as advocated by Breckinridge[14].

4.1 *Theory*

The shape of a thin circular plate of diameter D under uniform pressure P is given for $0 \le u \le 1$ to terms up to u^4 by

$$z = \frac{kP^{\frac{1}{3}}D^{\frac{4}{3}}}{E^{\frac{1}{3}}t^{\frac{1}{3}}} f(u) \tag{7}$$

where t is the thickness of the plate, E the modulus of elasticity and $u = 2x/D$, the fractional radial distance from the center of the membrane. For an inflated membrane of uniform thickness $k = 0.248$. Inserting the expression for f(u) to terms up to u^4 we obtain

$$z = \frac{0.248P^{\frac{1}{3}}D^{\frac{4}{3}}}{E^{\frac{1}{3}}t^{\frac{1}{3}}}\left[au^2 + (1-a)u^4\right] \tag{8}$$

For the classical Hencky equation a=0.9. The natural shape of an inflated membrane has higher order terms than u^4 because of an increasingly steeper upward slope near the periphery of the mirror.

Let us define the variation of membrane thickness as

$t = f(t,u) = t_0\{1 + Au^2 + Bu^4 + Cu^6 \ldots)$ (9)

We found that limiting t to the Au^2 term results in a parabolic thickness variation of special interest in practical regards. We then have

$$z = \frac{kP^{\frac{1}{3}}D^{\frac{4}{3}}}{E^{\frac{1}{3}}t_o^{\frac{1}{3}}\left(1+Au^2\right)^{\frac{1}{3}}}\left[au^2 + (1-a)u^4\right] \qquad (10)$$

whence the slope at z is then

Note that A is independent of P, E, t and central sag z of the inflated membrane. Solving for the value of A such that the u^3 term in Eq. 11 is zero at u = 1 we obtain A = 0.44 for

$$dz/du = \frac{kP^{\frac{1}{3}}D^{\frac{4}{3}}}{E^{\frac{1}{3}}t_o^{\frac{1}{3}}\left(1+Au^2\right)^{\frac{2}{3}}}\left[2au + 4(1-a)u^3 + 2Aau^3\right] \qquad (11)$$

the value of a = 0.9.

We can also evaluate A independently from slope data that include higher order terms in the $(1 + Au^2)$ terms that we neglected in Eq. 11. Note that setting A = 0.44 yields a paraboloid. One can select $A \neq 0.44$ so that the resulting membrane has a small u^4 term as would be required if the membrane were to serve as a convex hyperbolic Cass secondary. Likewise it could be selected so as to produce the aspheric shape of a Ritchey-Chretien primary mirror.

The sagitta of the inflated membrane, z, is then the integral of Eq. (11). Since there is no closed form for this integral it is necessary to evaluate it by numerical integration,

$$z = \Sigma\,(dz/du_i + dz/du_j)\Delta/2. \qquad (12)$$

4.2 *Example*

As an example let us take the case of a classical Hencky surface and a 6 μm membrane which under unspecified P and E had the following parameters:

$$dz/dx = 0.2375\,(1.8u + 0.4u^3). \qquad (13)$$

The results for the parameters for membranes of constant and variable thickness are shown in Table 1. The curve depths are from a numerical integration of the above equations and hence are only approximate in view of an integration step of 40 mm. The optimum value of A was determined by integrations of Eq (12) to be 0.42.

4.3 *Wavefront correction at a pupil*

Upgrading of a wavefront error that would otherwise limit system acuity is done by placing a wavefront corrector at a pupil[11]. The degree of correction that can be attained over a required field of view depends on the pupil minification factor, Q, which then sets the size of pupil that can manage a given wavefront aberration [12]. The approximate equation for the improvement factor possible at the wavefront correcting mirror is

$$C^{-1} = \frac{1}{\cos(\theta_1 \pm \phi)} - \frac{1}{c\cos(\theta_1)} - \frac{1}{\cos(\theta_2 \pm Q\phi)} + \frac{1}{\cos(Q\theta_2)} \qquad (14)$$

where θ_1 is the angle of incidence on the primary mirror, θ_2 the angle of incidence on the pupil mirror, ϕ the field angle and Q the pupil demagnification factor.

Table 2 shows the allowable input wavefront error for correction to an 0.1 μm output error for a typical 4-mirror Cass/Cass having an F/1 first stage and F/10 final focal ratio. The wavefront correction is applied at the quaternary for different pupil reduction factors, Q.

Table 2 Allowable input wavefront errors in um for an 0.1 μm output error [12]

	Wavefront correction pupil reduction factor, Q				
	5	10	20	50	100
FOV amin					
6'	1981	1654	943	233	63
12'	922	661	299	61	15
18'	574	366	145	27	6
30'	305	164	56	9	-
60'	118	50	14	-	-

From Table 2 we see that achieving a wavefront error reduction of 200 would permit upgrading a field of view of 6 amin at a pupil reduction factor of 50, e.g., a 10 cm pupil mirror for a 5 meter telescope. Correcting a 30 amin field of view on the other hand would require a 62.5 cm pupil mirror. The relationship between field of view and improvement factor for any value of Q is shown in Fig. 12.

5 Gores and pre-shaped membranes

There are two basic options for pre-shaping a membrane: 1) form a parabolic membrane by spin casting a polymer as discussed by Borra[15] or 2) make the membrane mirror from discrete pie-shaped gores. Making the membrane mirror from discrete pie-shaped gores offers an approach to make mirrors larger than can be made from a single sheet of polymeric material. Both provide a way to avoid the loss of reflectivity and increased scattering from the stretching of the aluminum or silver reflective surface. Such a mirror is fabricated by placing the appropriately edge-contoured gores on a convex surface and sealing adjacent panels by means of adhesive tape strips. The problem then is one of matching the inflation characteristics of the membrane and the membrane plus adhesive strips. The dependence of deflection on $t^{1/3}$ in Eq. 7, while mild, still shows a basic difficulty of the gore approach in equalizing the deflections of the membrane and of the membrane plus connecting strips. Much work has been done to solve the inflated shape problems caused by the added thickness at the sealing strips. The results are satisfactory at microwave wavelengths but far from acceptable even at thermal infrared wavelengths.

5.1 *Convex mold*

One option to pre-shape a monolithic membrane is to permanently deform a membrane by some appropriate means over a convex parabolic mold. The resulting parabolic membrane can now be inflated to the desired final focal length at a pressure considerably reduced over that required to deform a flat membrane to the same focal length. Even so, the paraboloid will be deformed by a Hencky term, but one that is accordingly smaller. To correct for this small Hencky term the mold must be modified so that this induced Hencky term is subtracted from the master. While this procedure could make a pre-shaped membrane that exactly compensates for the Hencky shape it poses a problem of how to attain the high degree of precision necessary that the inflated shape will be exactly as required. There is, however, a different solution that has natural properties that will tend to assure the required precision.

6 Fabrication of a variable thickness membrane

Fabrication is a key step in forming a membrane having a monotonically varying radial thickness gradient. Forming a uniform film by pouring a polymer onto a rotating flat plate has been done. One can modify the process to form a non-uniform membrane. We have shown above that the ideal radial variation in membrane thickness is parabolic. The process

for manufacturing such a parabolic thickness membrane to the desired high precision is to use a rotating table or mold.

There are two options for such a membrane: 1) a flat membrane having the required parabolic radial thickness gradient and 2) a parabolic pre-shaped membrane having the required parabolic radial thickness gradient. Both can be fabricated by relatively simple means.

6.1 *Flat membrane*

The equation given by Borra[16] for the rotation period T of a disc having a focal length f (independent of diameter D) of a liquid surface on a rotating table is

$$T^2 = \frac{8\pi^2 f}{g} \,. \tag{15}$$

Substituting $f = D^2/16\,z$ we obtain

$$T^2 = \frac{\pi^2 D^2}{2gz} \tag{16}$$

where the radial variation in thickness is given by

$$z = t_0\,(1 + Au^2)\,. \tag{17}$$

For a 1-meter diameter table and $t_0 = 0.01$ cm and $t = 0.0143$ at $u = 1$, $T = 59.3$ sec/ revolution. If one were to make a 20 meter diameter parabolic reflector for far infrared, for example, the rotation period for a membrane of thickness $t_0 = 0.10$ cm the rotation period would be $T = 377$ sec/rev.

Fig. 13 shows two options for forming a flat membrane having a parabolic radial thickness variation required to yield a paraboloid upon inflation. The first option (top) is to use a rotating table. A circular flat sheet of glass or other suitable material can be used for this table. A dike is placed at the periphery of the mold to contain the liquid polymer. The table is then rotated at an angular velocity such that the edge thickness at the planned diameter of the membrane (at $u = 1.0$) is 1.42 times the central thickness of the spun liquid as specified by Eqs. (15-17). The polymer is then polymerized while the table continues to spin.

An important advantage of using a polished master surface is that the optical surface of the finished membrane replicates the polished surface of the master. The free surface of the polymerized polymer on the other hand can have small surface irregularities that would affect the specularity of the finished membrane.

The second option (Fig. 13, bottom) is to use a fixed table and a slightly convex spherical master. The spherical curve produces the quadratic radial variation in thickness. This option would be preferred when one wants to make a number of identical flat membranes. The sag, s, of the master is given by

$s = h^2/2R$. Solving for R we obtain $R = h^2/2s$. (18)

For a 100 um central thickness membrane and a 1 meter diameter substrate the radius of curvature would be 880 meters.

6.2 *Curved membrane*

In view of the desirability to preserve the integrity of the reflective film deposited on the finished membrane one would like to reduce the amount of surface stretching to a minimum. This can be done by pre-shaping the membrane to a shape close to that required of the inflated mirror. The procedure is to form the mold by spin casting, upon which the membrane polymer is to be formed by spin casting at an angular velocity such that the required power of the membrane is obtained. One can use a polymer as reported by Borra[15]. Another option is to use glass, for example, as developed by Angel[17]. A third option is to use a low temperature metal. A fourth is to use a polymer atop a spin-set plaster substrate. In each case the membrane polymer needs to be separated from the mold by use of a suitable parting layer to ease removal of the membrane without damage.

The prior art has been to use spin casting to produce a uniform membrane. We add the additional requirement that it be spun at a slightly different velocity from that used to form the mold, the goal being to obtain a specific variation in radial thickness profile so that the inflated mirror is an accurate paraboloid.

The rotation period T of a liquid surface having a sagitta of depth z on a rotating table is given by Eq (16). We first form the mold surface, then add the liquid polymer. To change the edge thickness of the rotating parabolic surface by $z+\Delta z$ we need to change the rotation period by

$$\Delta T = \frac{\pi^2 D^2 \Delta z}{4gTz^2} \qquad (19)$$

As an example, for a 100 cm diameter F/1.1 membrane of central thickness 0.01 cm we have for the mold paraboloid

$$T = (\pi^2\ 110\ \text{cm} \div 980\ \text{cm/sec}^2)^{1/2} = 2.9770\ \text{sec/ rev.} \qquad (20)$$

To form a parabolic liquid surface of additional edge thickness of 0.0143 cm on this mold we need to change the angular velocity by ΔT seconds:

$$\Delta T = 0.0037\ \text{second, thus } (T + \Delta T) = 2.9807\ \text{sec/rev.} \qquad (21)$$

This small difference in rotation period emphasizes that attaining the required precision of rotation period may be a challenge.

In Fig. 14 (top) we illustrate the formation of a parabolic shaped membrane having a parabolic radial thickness gradient. The polymer is poured into the pre-fabricated mold paraboloid and spun at the slightly different angular velocity, as specified by Eq. (19), such that the edge thickness of the membrane is 1.42 times the central thickness at the periphery of the finished mirror, namely at u = 1.00. Note that u = 1 is not necessarily the same as the outer diameter of the inflated mirror for the reasons we have already stated.

Fig. 14 (bottom) shows the resulting parabolic membrane before and after inflation to the required focal ratio. The membrane mirror will attain a different central depth depending on the applied pressure. This pressure now has a different role from that with a flat membrane: it is the minimum necessary to smooth out the surface, not to form the shape of the membrane as in the case of a flat membrane.

The following example is for a small change in sagitta depth, from F/1.1 to F/1.0 and where P is the pressure to inflate a flat membrane from f = 100 cm to f = 110 cm:

$$z_0 = D^2/16\,f = 5.6818\ \text{cm.} \qquad (22)$$

The depth to change it from F/1.1 to F/1.0 is

$$z_1 = 6.2500\ \text{cm.} \qquad (23)$$

From the relationship between sagitta and inflation pressure in Eq (12) the ratio of pressures is then

$$P_1 = P_0 (z_1 / z_0)^3. \quad (24)$$

Thus the pressure would be changed to

$$P_1 = P_0 (6.25 / 5.6818)^3 = 1.33\ P_0. \quad (25)$$

This shows that a small change in final focal ratio requires a substantial pressure increment. One would therefore look for the smallest pressure change sufficient to smooth out the wrinkles in the membrane in transitioning from the folded stowed package to an operational mirror. Note, however, that the value of A = 0.42 for the thickness variation is unchanged since it is independent of pressure according to Eq. 11.

7 Practical aspects

One of several configurations of an inflatable optical system spacecraft that we have explored is shown in Fig. 15. The optical cavity is formed by a cylinder of inflated rings which position the secondary mirror and also provide a thermal shield. The planes of both the primary mirror and of the small secondary mirror are defined by the interface between two adjacent inflated rings. The carbon fiber metrology truss between the primary mirror and the secondary mirror to define and maintain focus and collimation is also shown.

The potential for a compact launch package shows the reason why continuation of work in inflatable optical systems is justified, the practical problems not withstanding. There are, however, a number of practical considerations that must be faced in successfully applying inflated membrane mirrors in the 0.5-12 um region. Here are some significant ones.

7.1 *Lifetime on orbit*

If inflation pressure must be maintained in order to keep the optical surfaces pristine a few micro punctures from meteoroid impacts become a concern. One would require a reserve of pressurized gas or a sublimable solid that could maintain a suitable pressure. This requirement emphasizes that the lowest operating pressure is a priority, hence the choice of a pre-shaped membrane as discussed above. Alternately one could risk an unpredictable lifetime in exchange for a very low-cost readily replacable spacecraft. The equations and a detailed discussion of issues relating to the influence of micrometeorites have been given by Rapp[8].

7.2 *Focus and collimation*

Maintenance of focus and collimation in an inflatable optical system is a challenging issue, in particular the effect of small changes in pressure affecting focus. Breckinridge[14] has suggested using carbon fibers to provide the basic truss defining the relative positions of the optical elements and focal plane as a way to avoid this sensitivity to pressure as well as thermal gradients in the inflatable envelope.

7.3 *Peripheral tensioning*

A word of caution: as far as we can determine all measurements of inflated membrane mirrors have been done using a single surface and deforming it by reducing the pressure in the unit holding the membrane fixed to the periphery of a flat, very rigid metal ring. For space applications such a heavy defining ring cannot be used. For such applications an inflatable mirror consisting of the two surfaces joined at their periphery requires an inflated tensioning ring plus a tensioning web. Without a tensioning ring the periphery of the inflated mirror will contract until a new equilibrium is established, one with an accentuated turned-up periphery. An aluminum membrane party balloon illustrates the tendency of an inflated mirror to develop a sharply turned up periphery, the angle between the two sheets at the junction tending towards 180°.

Problems arise in attaching the mirror to an inflated stiffening ring. For microwave antennae a network of rope stays is often used to knit the mirror to the ring at a number of closely spaced but discrete locations. These points of attachment produce localized surface errors that are large compared to visible wavelengths. Attaching the mirror to the inflated stiffening ring by means of a continuous sheet has its problems also. The seal between the two membranes of the mirror must be accurately circular and the inflated tensioning ring highly planar, both of which are very real challenges.

7.4 *Departure from the Hencky surface*

In view of the above issues the equation for the Hencky surface found for the membrane mirror in the example above may be considerably different. In fact the coefficients of the traditional Hencky equation (Eqs. 7 and 8) $a = 0.9$, $(a - 1) = 0.1$ depend on the outer boundary, u, of the mirror relative to the physical boundary of the inflated membrane. This is because the up-turned edge increases in severity as the physical boundary is approached, requiring significant u^6 and u^8 terms. Thus the value of $A = 0.42$ in Eq. 10 applies only to a surface described by $a = 0.9$. For any real membrane one must first

determine the applicable coefficient a, which depends on the focal ratio of the mirror, the membrane thickness and the outer useful diameter of the inflated mirror.

In addition to these departures one faces localized variations in modulus of elasticity that become readily apparent when one observes a sightly out of focus image of a point source. It therefore may be necessary to correct for these in making the wavefront corrector that would be placed at a minified pupil within the optical configuration.

7.5 *Reflective coating*

Another serious issue is that when an aluminized sheet is stretched the reflective coating beaks up into islands with clear gaps in between. Rapp[18] cites work at ILC, Dover, Inc., that shows that due to the nature of the aluminized coating on the Kapton film an elongation "greater than 5% the aluminum coating would disseminate" leading to transmission of light through the reflective surface. We encountered this problem years ago when we shaped concave solar concentrator mirrors out of flat sheet material that had been aluminized. The reflectivity decreased and the scattered light sharply increased. In the example membrane mirror above, the stretch of the inflated membrane increases its surface area by 10.4%. This indicates that the reflectance would be decreased by this same amount assuming that the reflective film prefers to fracture rather than stretch. The solution to this problem is to use a pre-shaped membrane so that the amount of stretching is minimized.

7.6 *Optical window membranes*

An inflatable membrane mirror requires a window that is optically satisfactory and transparent to the passbands to be used. A number of investigators have examined transparent membranes for suitability for the optical window of an inflatable membrane mirror. All have found optical path errors that make their use doubtful for a diffraction-limited system. The effects range from optical path small-scale effects like discrete striations to large-scale thickness variations. The large-scale effects can in principle be taken out by the wavefront corrector mirror.

7.7 *Removal from a parabolic mold*

The major practical issue is how to remove the polymerized membrane from the mold surface, especially a deep parabolic mold. Adhesion poses a difficulty since removal requires that an air film creep in between the membrane and the mold. Applied removal forces must be kept low so that a permanent deformation of the membrane is avoided.

One option for how to solve this problem is to form the upper layer of the parabolic mold from a material with a low melting point but which remains solid at the temperatures involved in polymerizing. An example is Wood's metal, which has a melting point under the boiling point of water. Then removal of the membrane would involve simply heating the mold to 100°C whereupon the liquid metal would float the finished membrane.

Another option would be to place a passage for air at the center of the mold. After finishing the membrane air pressure could be used to gently lift it free of the mold, starting at the center and propagating outward.

8 Conclusions

A number of conclusions can be drawn from this analysis.

1) Deliberate variation of the radial thickness can create a membrane that will be an accurate paraboloid upon inflation. A value of $A = 0.42$ is found for the au^2 thickness profile term independent of thickness or inflation pressure.

2) Selection of a slightly different value for A can yield the specific hyperbolic shape as required for a convex Cassegrain secondary or a Ritchey-Chretien primary mirror.

3) The required membrane having a radial parabolic variation in thickness can be produced either by spin casting on a flat surface or spin casting on a pre-formed parabolic mold.

4) Commercial Mylar of 1983 vintage has enough variation of physical properties with azimuth that an inflated 6 um thick Mylar membrane mirror will have astigmatic behavior of such a magnitude that it is doubtful if it can be used in a high-acuity optical passband system. Other polymers, like Kapton, may alleviate this problem.

5) Practical application of inflatable membrane mirrors has significant issues that must be faced and solved. The potential advantage of low cost large aperture space telescopes for use in the 0.5 to 12 μm region hangs in the balance.

Acknowledgments

We wish to acknowledge the discussions we have had with our JPL associates: Celeste M. Satter in discussions of inflatable mirrors and structures and the possibility of using preshaped uniform membranes as an alternate approach to variable thickness; Gregory H. Smith for his exploration showing the difficulty of integrating the Hencky curve into a wide field visible passband optical system; Donald Rapp for his comprehensive review of the subject and hard-to-find references that we have used to give credits for prior art; to Dan Marker of AFRL for his tutorial help by providing us a manuscript on their work on inflatable mirrors; and to James B. Breckinridge for his leadership and important contributions in searching for new approaches toward a viable inflatable membrane mirror optical system.

The research described in this paper was carried out by the Jet Propulsion Laboratory, California Institute of Technology, under a contract with the National Aeronautics and Space Administration.

References

1 C. W. Tolbert and A. W. Straiton, "A 16-foot Millimeter Wavelength Antenna System, Its Characteristics and Its Applications," *Proc. IEEE* , 225-229 (1964).

2 R. E. Freeland and G. D. Bilyew, "IN-STEP Inflatable Antenna Experiment," Paper No. IAF-92-0301, *Proc. 43rd Congress, Int. Astronautical Fed, Washington, D. C.* (1992).

3 C. S. Taylor, *Proc. Solar En. Conf, Dhahran, Saudi Arabia, 1975*, Ed. A. Kettani, UPM, Dhahran, Saudi Arabia (1976).

4 A. B. Meinel and M. P. Meinel, "Mirror Collector Optics," *Applied Solar Energy*, 185-187, Addison-Wesley, Reading Mas. (1978).

5 W. R. Clayton, and P. A. Gierow, Inflatable Concentrators for Solar Thermal Propulsion, *ASME Solar Engineering*, **2**, 795-800 (1992).

6 H. Hencky, "Uber den Spannungszustand in kreisrunden Platten," *Z. Math. Phys. 63*, 311-317 (1915).

7 J. B.Breckinridge, A. B. Meinel and M. P. Meinel, "Inflation-deployed camera," *Proc. SPIE Conf. 3356*, 780-788, **3356**, (1998).

8 D. Rapp, "Prospects and Limitations of Technical Approaches for Ultra Lightweight Space Telescopes," *JPL Internal Document D-13975* (30 Sep. 1996).

9 G. Veal and M. Thomas, "Highly Accurate Inflatable Reflectors," *L'Garde, Inc., Final Report, AD-A143628* (1984).

10 G. Veal, "Highly Accurate Inflatable Reflectors—Phase II," *L'Garde, Inc., AFRPL Report, No. TR-86-089* (1987).

11 C. Cassapakis, letter, undated, with data sheets from measurements dated 12/6/83.

12 A. B. Meinel and M. P. Meinel, "Two-stage optics: high acuity performance

from low-acuity optical systems," *Opt. Eng*, **31**(11), 2271-2281 (1992).

13 A. Palisoc, G. Veal, C. Cassapakis, G. Gresechik and M. Mikulus, "Geometry attained by pressurized membranes," *Proc .SPIE Conf. 3356*, 747-758, **3356** (1998).

14. J. B. Breckinridge, discussions at Jet Propulsion Laboratory re inflated mirrors for optical passband applications.

15 E. F. Borra, R. Content, L. Girard, S. Szapiel, L. M. Tremblay, "Liquid mirrors - Optical Shop Tests and Contributions to the Technology", Astrophys. Journal, 393 (2), 829-847 (1992).

16 E. F. Borra, "Liquid Mirrors," Proc. Int. Workshop on Mirror Substrate Alternatives, Ed. J. P. Rozelot & W. Livingston, OCA/CERGA, Grasse, France, 211-216 (199?) .

17. J. R. P. Angel, "8-m Borosilicate Honeycomb Mirrors," *Very Large Telescopes and their Instrumentation, ESO Conference and Workshop Proceedings No. 30*, ESO, Garching, Ed. M.-H. Ulrich, 281-300 (1988) .

18 D. Rapp, "Prospects and Limitations of Technical Approaches for Ultra Lightweight Space Telescopes," *JPL Internal Document D-13975*, 3-12 (1996).

FIGURE CAPTIONS

Fig. 1 The caustic formed by the membrane mirror analyzed in this paper. A secondary mirror must be located sufficiently far from the start of the caustic in order to handle the aberrations of a Cassegrain system.

Fig. 2 Two examples of measurements of inflated membrane mirrors showing an asymmetrical W-curve .

Fig. 3 The tabulated data minus a paraboloid (smooth curve) and as corrected for metrology coordinate alignment coma (curve with dots).

Fig. 4 Data for the 6 um Mylar membrane mirror, the sagitta (top) and the difference with respect to a paraboloid (bottom).

Fig. 5 Slopes measured along an azimuth (top) and after subtraction of the parabolic slope (bottom) with the cut reversed and superimposed to permit full correction for the metrology zero point.

Fig. 6 The mean curve from Fig. 3 reversed and superimposed (top) with the difference showing a 3.5 μm rms (bottom), close to the difference of one in the last place of the original measurement data.

Fig. 7 Comparison of the residuals after subtraction of the same parabolic curve from both azimuths shows that there is a significant difference in the modulus of elasticity in these orthogonal directions.

Fig. 8 The direct and reversed curves for both azimuths superimposed showing a spread of curves at large radial zones.

Fig. 9 Schematic representation of the type of astigmatism caused by a variation of the membrane value of E (or thickness t) in orthogonal directions showing a 90° change in the major axis between the inner and outer regions of the mirror surface.

Fig. 10. Variation of the membrane slopes vs. zonal radius, r, for a uniformly thick membrane (large circles) and a variable thickness membrane (small circles) with a linear (parabolic) relationship shows the ability to control the surface figure by increasing the membrane thickness with increasing radial distance.

Fig. 11 The residual between the variable thickness membrane and the straight line relationship of Fig. 10 showing that a moderate dependence on thickness on u^4 and u^6 is present.

Fig. 12 The inter-relationship between field of view and required improvement factor defines the required pupil demagnification factor Q.

Fig. 13 Two fabrication modes: 1) a flat table carrying a flat sheet of glass is spun so that the edge thickness of the liquid polymer is that required to produce the edge thickness as illustrated above and 2) a convex spherical polished master on which the liquid polymer is poured.

Fig. 14 The sequence shows the fabrication mode for forming a membrane having a parabolic radial variation in thickness (top). The added curve depth after inflation produces the required focal ratio of the mirror (bottom).

Fig. 15 Schematic cross-section of an inflatable space telescope using inflated rings plus metrology fibers to locate the position of the secondary mirror, showing the compactness that is possible using an inflated membrane mirror and associated structure.

Fig. 16 The arrangement for laboratory measurements (top) and space applications (bottom) is different. In order to predict on-orbit performance, analyses based on laboratory measurements will require appropriate modifications.

TABLE CAPTIONS

Table 1 Parameters for membranes of constant and variable thickness.

Table 2 Allowable input wavefront errors in um for an 0.1 μm output error [12].

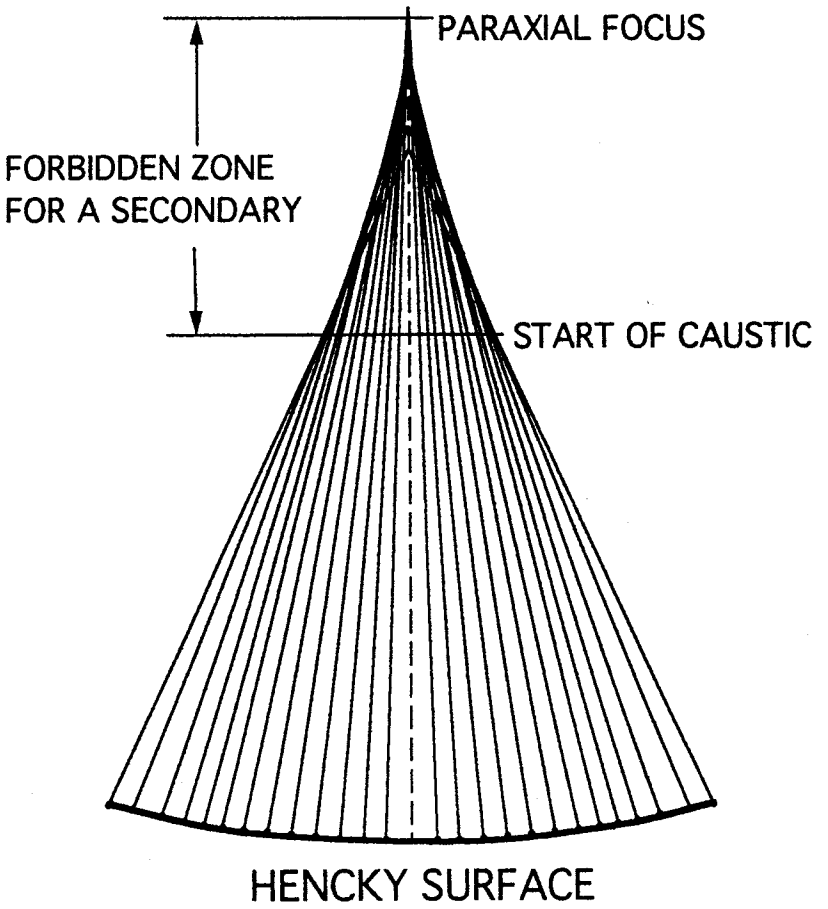

Meinel & Meinel Fig. 1

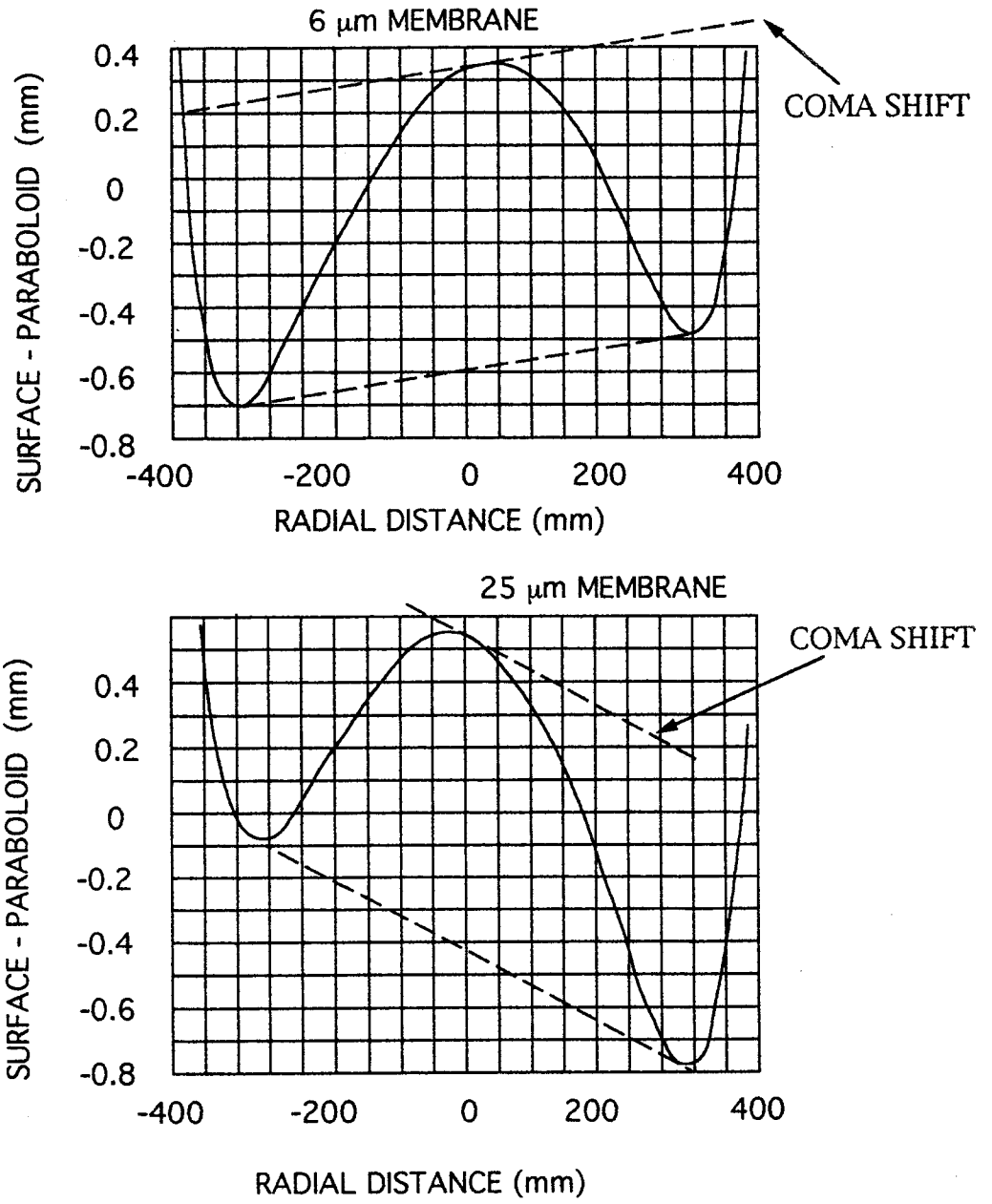

Meinel & Meinel Fig. 2

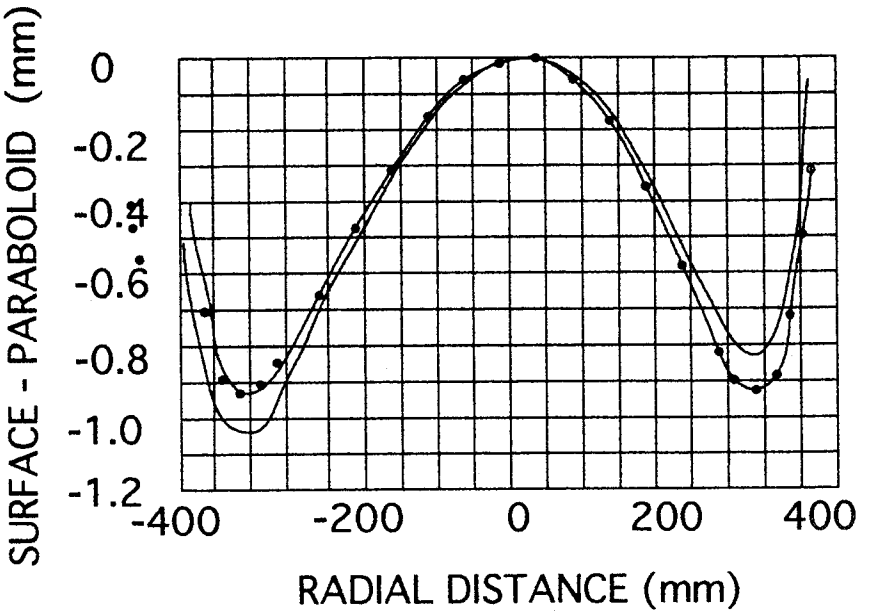

Meinel & Meinel Fig. 3

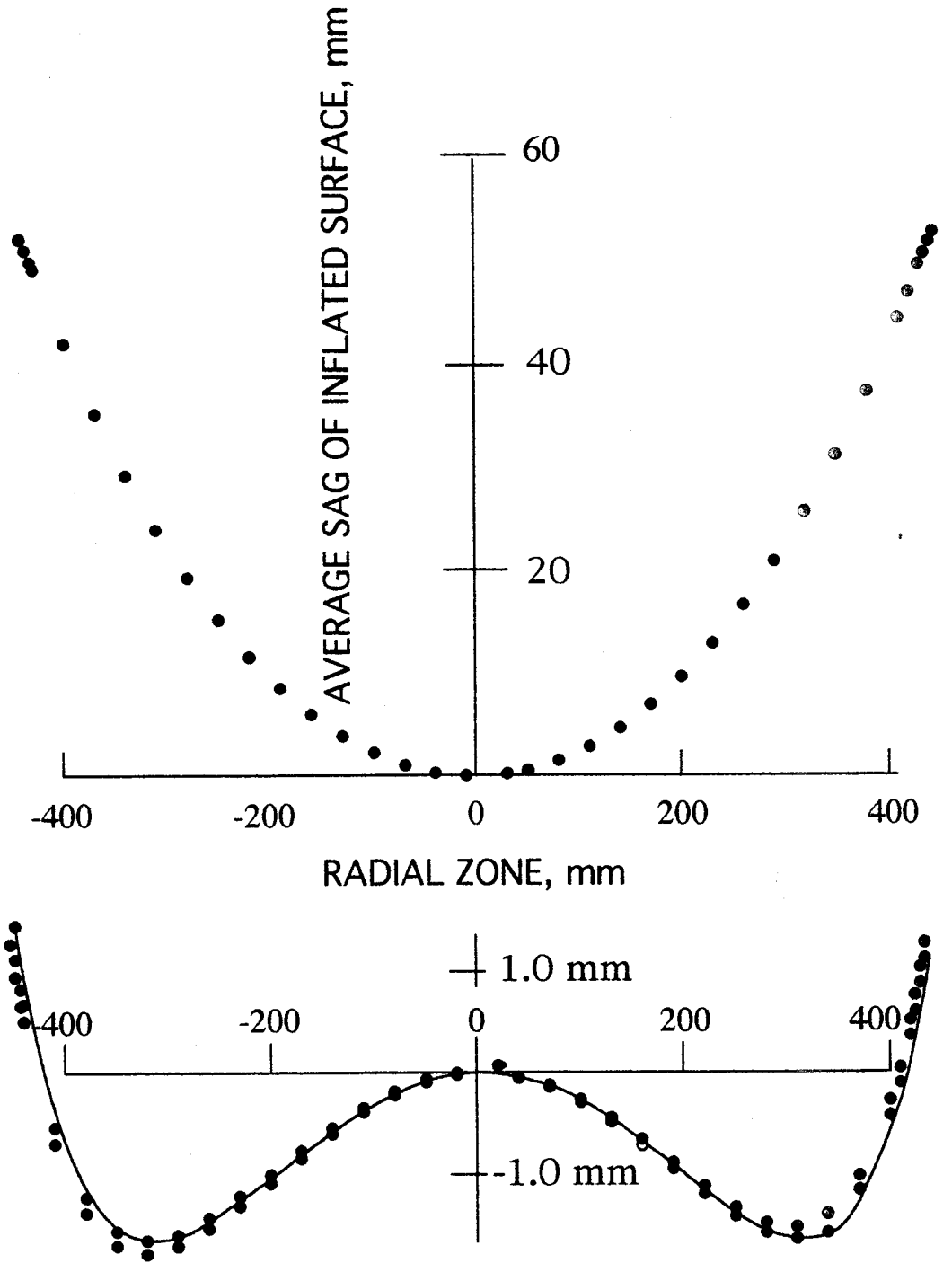

Meinel & Meinel Fig. 4

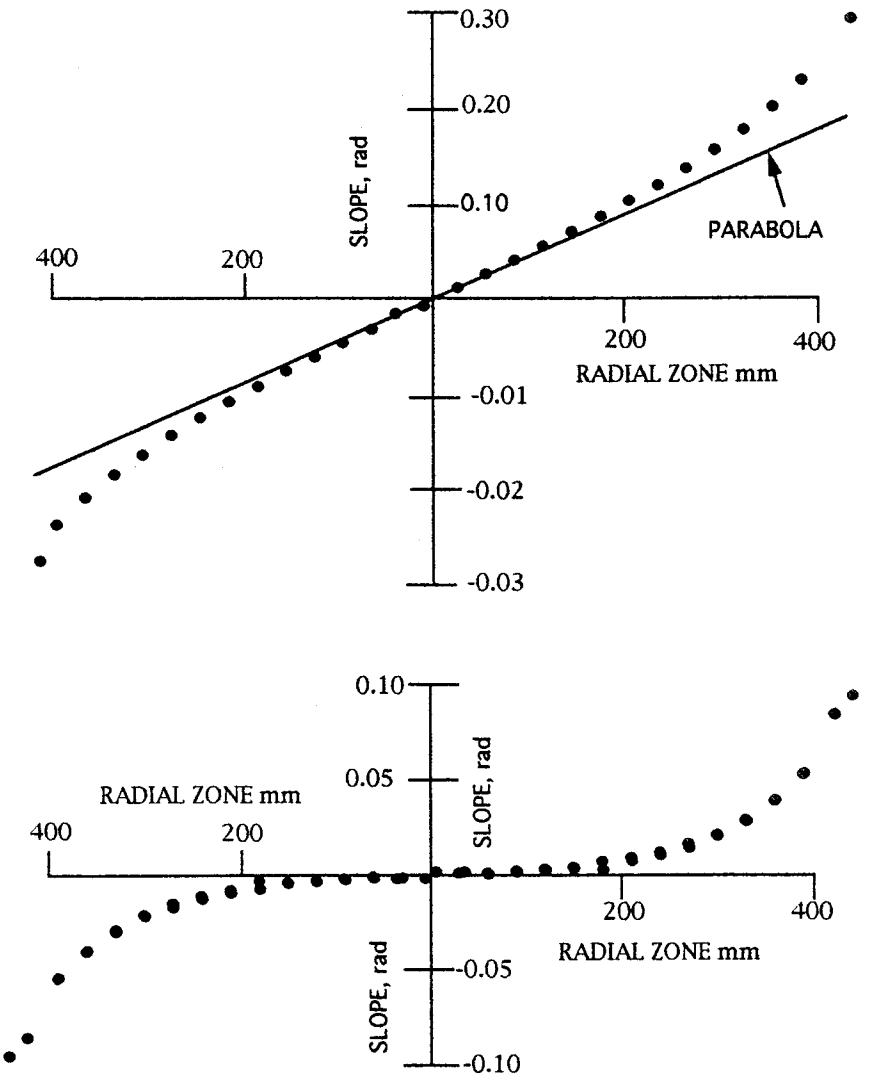

Meinel & Meinel Fig. 5

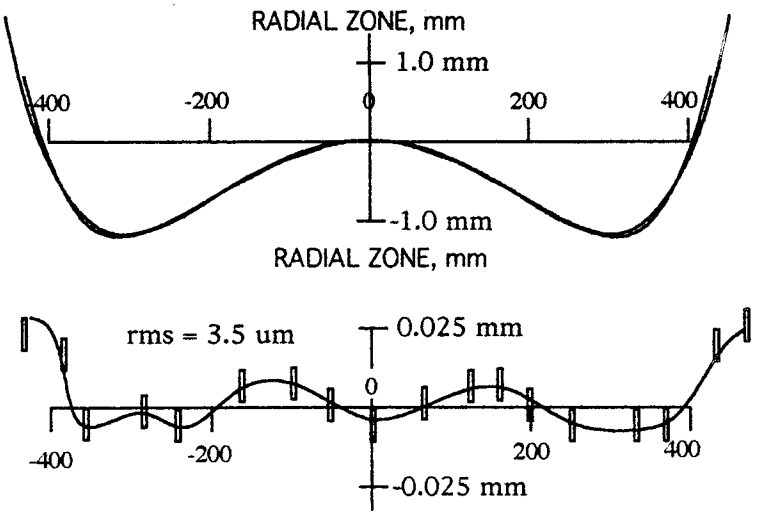

Meinel & Meinel Fig. 6

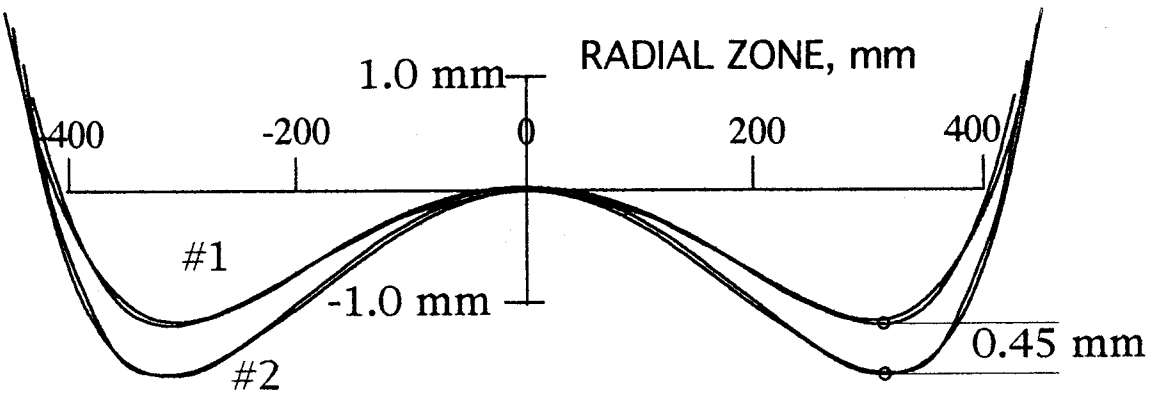

Meinel & Meinel Fig. 7

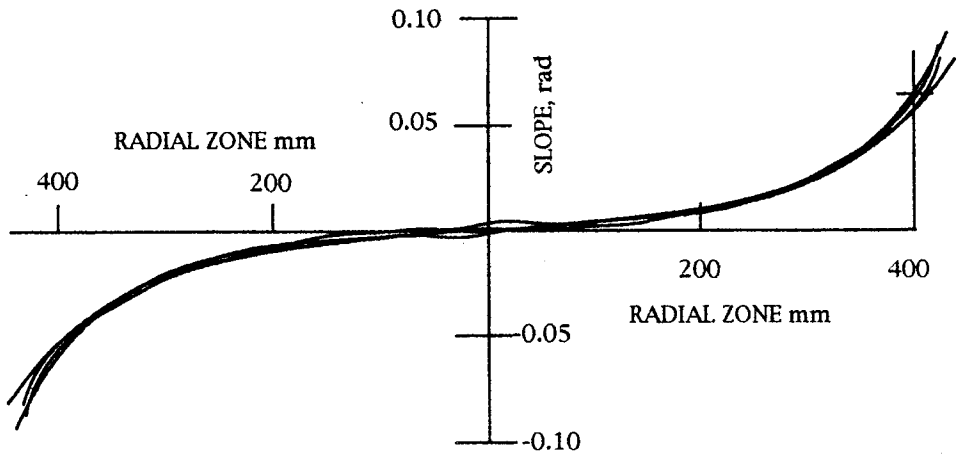

Meinel & Meinel Fig. 8

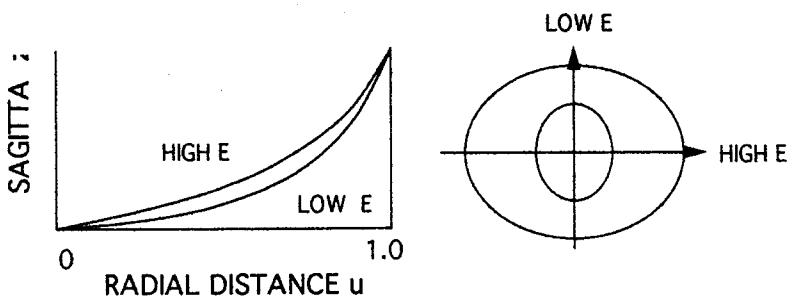

Meinel & Meinel Fig. 9

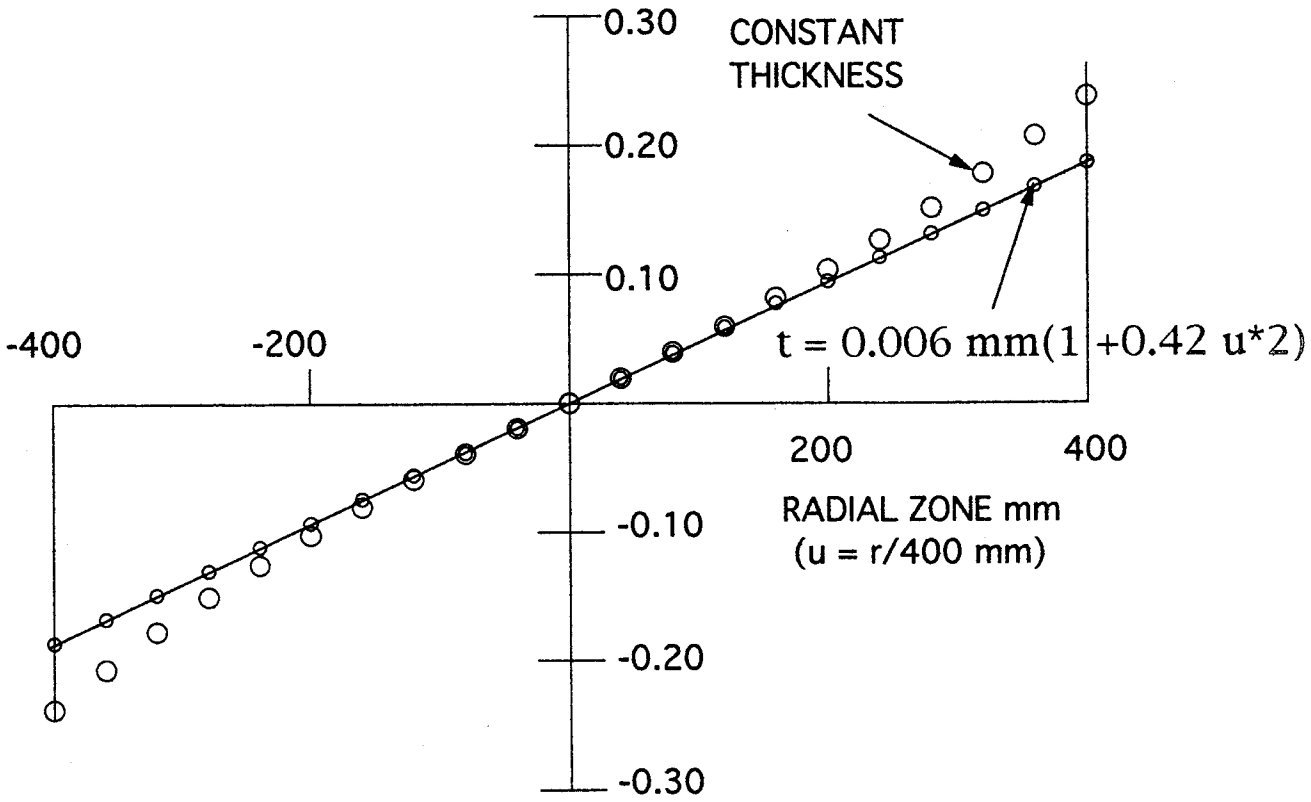

Meinel & Meinel Fig. 10

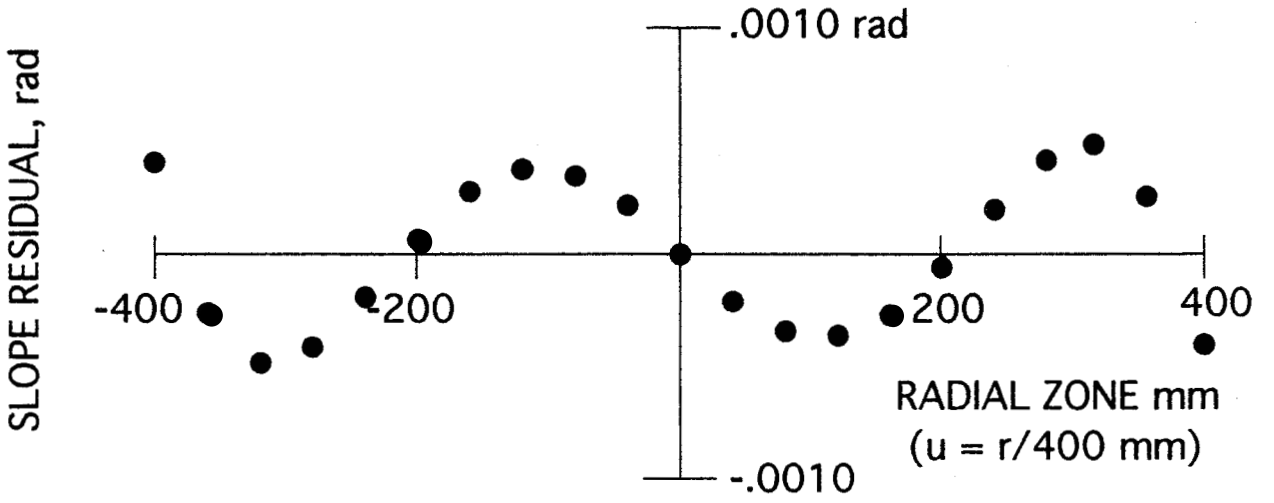

Meinel & Meinel Fig. 11

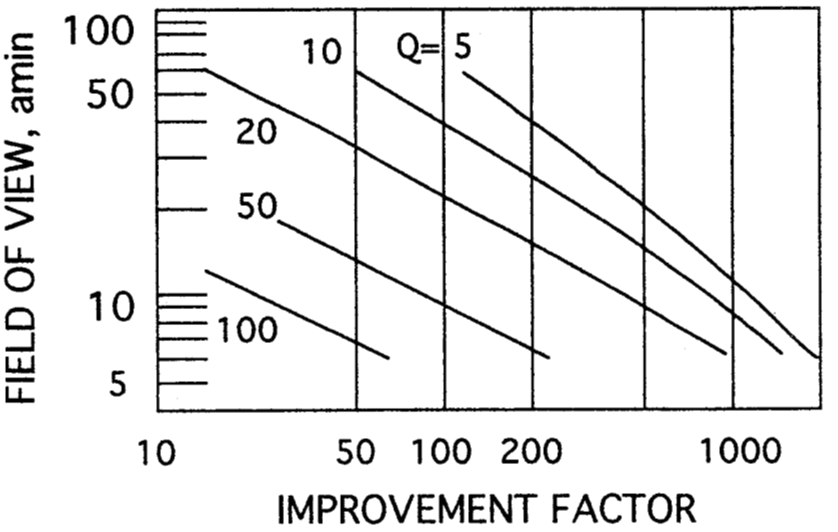

Meinel & Meinel Fig. 12

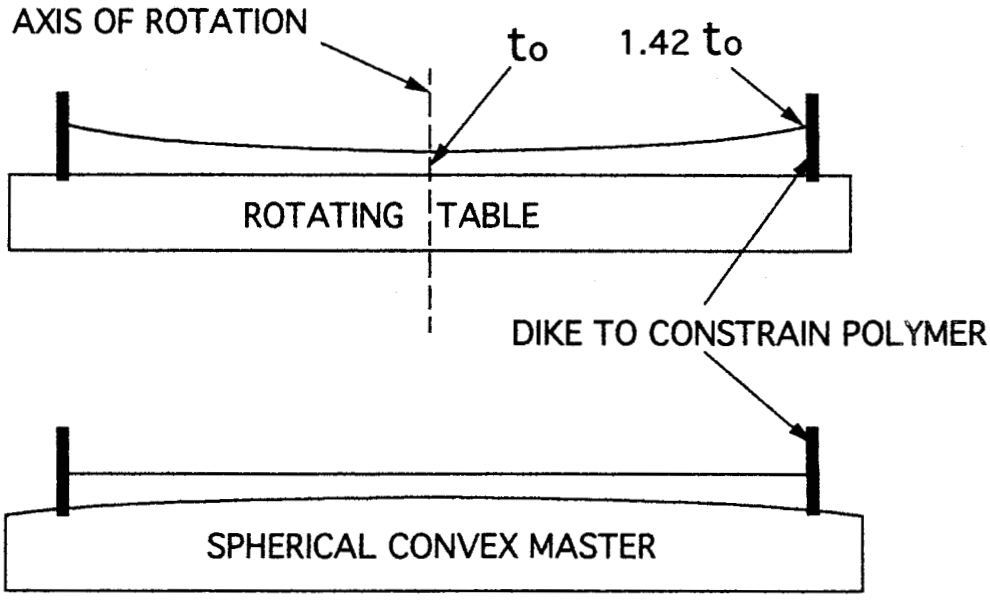

Meinel & Meinel Fig. 13

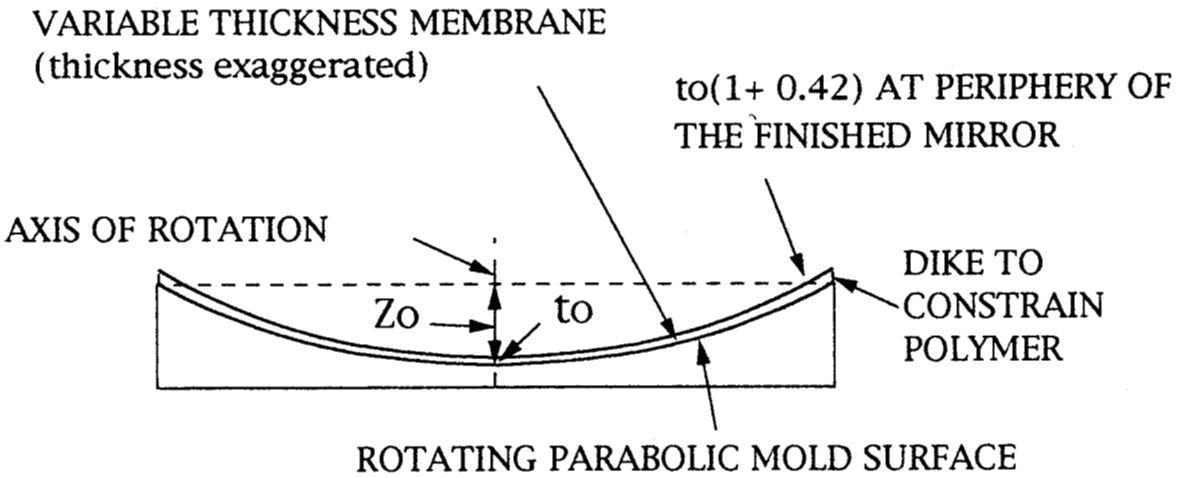

PRE-CURVED MEMBRANE FABRICATION MODE

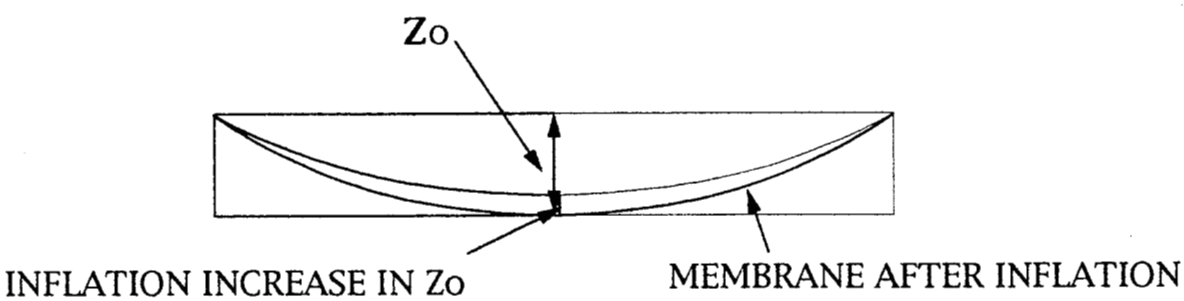

Meinel & Meinel Fig. 14

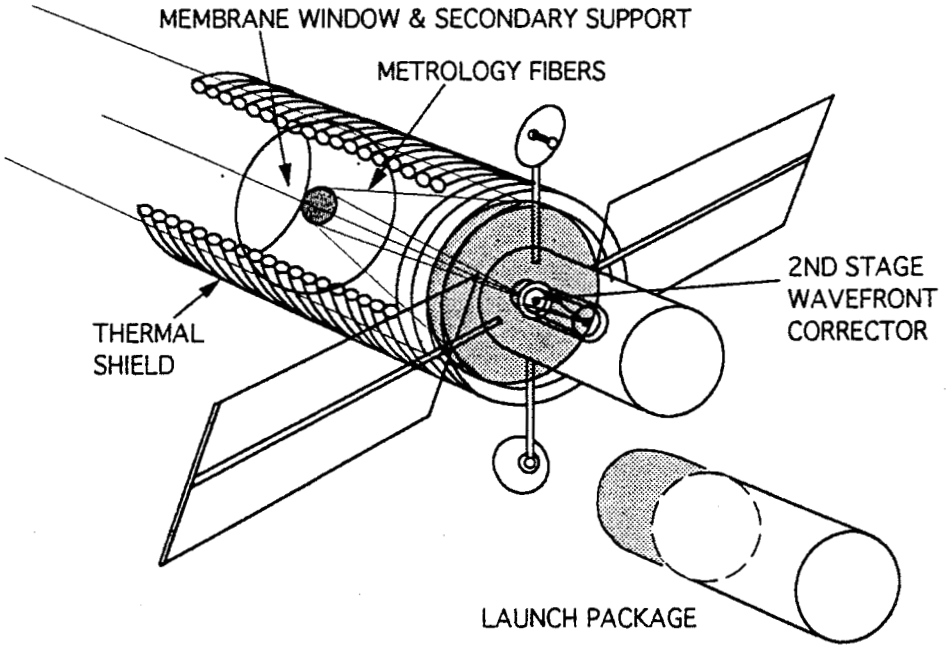

Meinel & Meinel Fig. 15

Aden Baker Meinel received his BA degree (1947) and PhD degree (1949) in astronomy, University of California, Berkeley, and honorary DSc degree (1990) from the University of Arizona. He was associate director of the Yerkes and McDonald Observatories and the founding director of the Kitt Peak National Observatory. At the University of Arizona he was chairman of the Astronomy Department, director of the Steward Observatory and the founding director of the Optical Sciences Center (the Meinel Building). He was Distinguished Scientist, Jet Propulsion Laboratory, California Institute of Technology (1985) and in retirement is Sr. Member, Technical Staff-Principal, On-Call. He has published 5 books, 18 book chapters, and 179 papers on optics, astronomy, upper atmospheric phenomena and solar energy, and was the discoverer of the Meinel molecular band systems of OH and of $N2^+$.

Marjorie Pettit Meinel received her BA degree in astronomy (1943), Pomona College and MA degree in astronomy (1944), Claremont Colleges. In 1944 she began her career as Research Associate at the California Institute of Technology, Navy rocket project. After raising her seven children she joined the Optical Sciences Center, University of Arizona (1971), as Research Associate. She was member, Technical Staff, Jet Propulsion Laboratory, California Institute of Technology (1985) and in retirement is member, Technical Staff, Senior Engineer, On-Call. She has published three books, eight book chapters, and 96 papers on optics, astronomy, upper atmospheric phenomena, and solar energy. Marjorie and Aden Meinel were married in 1944.